

## Continuous Time Least Square PI Control Method for Quasi-Z Source Inverter

Özkan ÖZKARA\*, Ahmet KARAARSLAN

**Abstract:** This paper presents the proposed model of proportional Integral (PI) controller using continuous time least square method (CT-LSM) for a quasi-Z source inverter (qZSI). PI control is one of the most applicable control methods in power systems. Then, CT-LSM is mainly a statistical optimization method including parameter estimation for nonlinear systems to control. The proposed model is designed to set a control structure without using the nonlinear loads of qZSI and also improve PI control applications against the nonlinear system dynamics. Controller design for qZSI is divided into two parts which are explained as dc side and ac side in both two mode operations. For the dc side of the system, PI controller is designed according to approved system and its estimated parameters which are calculated from state space analysis of qZSI. As for the ac side, the voltage and current regulations are controlled in order to transfer the power to inverter legs based on design criteria. Simulation results by using the current qZSI model on Matlab/Simulink are used to research and analyze the effectiveness and efficiency of the proposed control design.

**Keywords:** continuous time least square method; quasi Z source inverter; system estimation

### 1 INTRODUCTION

Power converters have been designed to manage maximum energy collecting and power processing for using a green, renewable, and independent energy source because fossil fuels are scarce and we are becoming more and more dependent on renewable sources to meet the rising global energy demand. Buck, boost and buck-boost derived topologies can be used by regarding the need of output voltage [1]. As a solution, novel power electronics topologies within switch mode power supplies (abbreviated as SMPS) have been investigated and have increased in popularity. SMPSs are used in many applications, such as generation resources, hybrid electrical vehicles, battery backup systems for uninterruptible power supplies, and LED lighting systems [2].

Depending on their applications, the performance of SMPS becomes critical issue. Therefore, stability analysis and stabilization problems for switched systems have been extensively studied [3]. Impedance source inverters have been investigated for new-generation inverter topologies, which offer significant advantages in a single stage without requiring additional switching devices [4]. To obtain proper performance of the SMPSs, as an interface between power source and application area, ZSI provides an attractive feature for one-stage power conversion with simultaneous buck-boost ability [5]. It reduces the power consumption and cost of the control system, improves efficiency, and accelerates the system dynamic response [6].

The Z-source inverter (ZSI) was proposed as an alternative to the traditional DC-AC converter [7]. With its voltage buck/boost properties, the ZSI can overcome input voltage variables in a wide range, although it is generally yielded by a two-stage including DC-DC converter and DC-AC structure. With the low cost and high reliability due to shoot-through state, there has been attention in ZSI and its several applications. Without the use of extra switching devices, the ZSI concept uses an x-shaped configuration of inductors and capacitors to achieve voltage buck/boost in a single step. Shoot-through state (ST) is harmed by the energy that is released from inductors' stored energy. The voltage increase is then

established at the non-shoot-through (NST) state. Pulse-width modulation (PWM)-based voltage boost techniques have been initially researched as various control structures and approaches for ZSI.

Then, a qZSI shown as in Fig. 1 has been proposed for power applications. It has fewer harmonic contents, greater buck/boost characteristics, and the ability to control the phase angle output. It does not require the filter, and has high power performance characteristics over the conventional inverter [8]. It can utilize the shoot-through (ST) state to boost the input voltage, which improves the inverter reliability and increases its application field [9]. The qZSI operates in two modes alternatively as continuous conduction mode (CCM) and discontinuous conduction mode (DCM). In addition, the voltage boost and ac inversion functions can be combined into one power conversion stage [10].

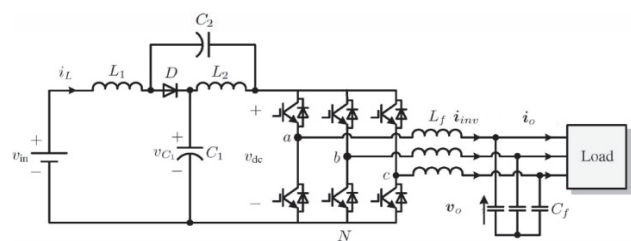


Figure 1 General Structure of Three Phase Quasi Z Source Inverter

By evaluating both steady-state and dynamic performances, the design of qZSI is examined. By putting state-space and closed-loop controllers into practice, the dynamic model and transient analysis of qZSI are examined. The control variables,  $d_{sth}$  (shoot-through duty ratio) and  $M$  (modulation index) which provides the power balance between input and output of the inverter [11] of the qZSI, should be considered.

Therefore, many control approaches such as proportional including sliding mode control, neural network, and fuzzy control [12-13] have been constructed to qZSI. These control strategies have been successfully applied to grid-connected inverters with improved performance [14]. PI control based on PWM technology is widely applied [15] to the impedance source network inverter's control method. PI control is a linear control

technique that has a slow rate of adjustment and weak resilience. Although the system can achieve a control effect with faster response and less fluctuation after a long period of repeated adjustment of the parameters of the PI regulator, it often takes a lot of time during the debugging process, and the output of the PI regulator is often saturated or fluctuates greatly [16-17].

For nonlinear systems, parameter estimation of the continuous-time systems with time delays has received particular attention during the past decades [9]. Parameter estimation is expressed as an optimization problem that measures the error value between the expected output in a sampling time sequence of a cost function and the observed system output measurements. To solve the estimation problem involving linear systems with a single delay and no other unknown parameters, many computational methods have been proposed [18-19]. This algorithm is further extended to more general nonlinear systems [20-21].

Consequently, parameter estimation can be a property for control approach since qZSI includes nonlinear circuit elements such as capacitors and inductors. These nonlinear parameters affect directly characteristic equation of qZSI which is yielded from steady state analysis. Then small signal modelling and dynamic approach are determined by obtaining relations among voltage current, ST duty cycle. To develop PI control of qZSI, in this way, a system equation is approved similar to the small-signal equation of the system. Second, this equation is estimated using continuous time least square method (CT-LSM) and converges to the real system parameters. Finally, the PI controller parameters are determined in accordance with the estimated system. Therefore, qZSI has been implemented by improving the robustness and fast dynamic response against unintended variations during operation.

The thorough modeling and control difficulties of the qZSI to be used in low power applications are further examined in this study. By using small-signal analysis, the dynamic model of the quasi-Z-source network is created. System features are thoroughly examined to determine the ideal component parameter and operating state of the system. A brand-new control technique called Continuous Time Least Square Method (CT-LSM), which can be applied across a wide voltage variation range, is suggested based on the dynamic model.

## 2 MODELLING OF QUASI-Z SOURCE INVERTER

Fig. 1 shows the circuit configuration of qZSI. The qZSI has two inductors  $L_1$  and  $L_2$ , and two capacitors  $C_1$  and  $C_2$ . Each capacitor and inductor is chosen with an equal value. The continuous conduction mode (CCM), also known as the shoot-through state and the non-shoot-through state, has two operating states for the qZSI. The total switching cycle time is called as  $T$ , which consists of the shoot-through cycle time and non-shoot-through cycle,  $T_0$  and  $T_1$  respectively. Therefore, the shoot through duty ratio is calculated as  $d_{sth} = T_0/T$ . Generally,  $d_{sth}$  is called as "D".

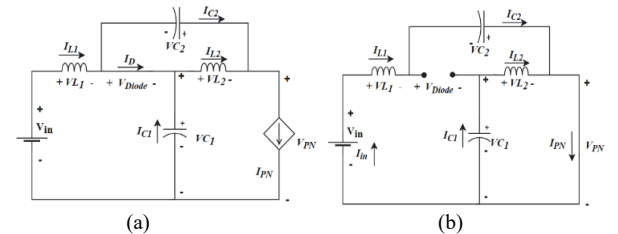


Figure 2 States of qZSI for: a) Shoot-through state, b) Nonshoot-through state

The DC part of the inverter passes to short-circuit with the upper and lower switches during the shoot-through state. Fig. 2a, shows the qZSI in the shoot-through state. From shoot-through equivalent circuit.

$$\begin{aligned} I_{C1} &= -I_{L2} \\ I_{C2} &= -I_{L1} \\ V_{L1} &= V_{C2} + V_{IN} \\ V_{L2} &= V_{C1} \end{aligned} \quad (1)$$

State space form of ST from Eq. (1) is given in Eq. (2) and Eq. (3);

$$\dot{X} = A_1 X + B_1 U \quad (2)$$

$$x = \begin{bmatrix} i_{L1} \\ i_{L1} \\ V_{C1} \\ V_{C1} \end{bmatrix}, A_1 = \begin{bmatrix} -R/L & 0 & 0 & 1/L \\ 0 & -R/L & 1/L & 0 \\ 0 & -1/C & 0 & 0 \\ -1/C & 0 & 0 & 0 \end{bmatrix}, B_1 = \begin{bmatrix} 1 \\ L \\ 0 \\ 0 \end{bmatrix}, u \begin{bmatrix} i_{out} \\ V_{in} \end{bmatrix} \quad (3)$$

The inverter functions like a typical voltage source inverter when it is not in the shoot-through state. The qZSI is depicted in the non-shoot-through state in Fig. 2b. Using the comparable circuit without a shoot-through.

$$\begin{aligned} I_{C1} &= I_{L1} - I_{DC} \\ I_{C2} &= I_{L2} - I_{DC} \\ V_{L1} &= V_{IN} - V_{C1} \\ V_{L2} &= -V_{C2} \end{aligned} \quad (4)$$

State space form of NST from Eq. (4) is given in Eq. (5) and Eq. (6);

$$\dot{X} = A_2 X + B_2 U \quad (5)$$

Then two states are solved together and the equation is given below briefly.

$$x = \begin{bmatrix} i_{L1} \\ i_{L1} \\ V_{C1} \\ V_{C1} \end{bmatrix}, A_2 = \begin{bmatrix} -R/L & 0 & 0 & 1/L \\ 0 & -R/L & 1/L & 0 \\ 0 & -1/C & 0 & 0 \\ -1/C & 0 & 0 & 0 \end{bmatrix}, B_2 = \begin{bmatrix} 1 \\ L \\ 0 \\ 0 \end{bmatrix}, u \begin{bmatrix} i_{out} \\ V_{in} \end{bmatrix} \quad (6)$$

$$\begin{aligned}\mathbf{A} &= D \times A_1 + (1-D) \times A_2, \\ \mathbf{B} &= D \times B_1 + (1-D) \times B_2\end{aligned}\quad (7)$$

For ideal qZSI, internal resistance of capacitors and inductors is ignored and the steady state solution given as below.

$$\begin{aligned}V_{PN} &= \frac{V_{in}}{1-2D} \\ V_{C1} &= \frac{(1-D)V_{in}}{1-2D} \\ V_{C2} &= \frac{-DV_{in}}{1-2D} \\ I_{L1} = I_{L2} &= \frac{(1-D)i_{out}}{1-2D}\end{aligned}\quad (8)$$

where  $V_{PN}$  represents the total voltage of capacitors in DC side.

## 2.1 Small Signal Modelling and Dynamic Approach of Quasi Z Source Inverter

$D$  and  $V_{in}$  are subjected to a modest disturbance in order to analyze a small-signal model of q-ZSI. Small signal variations in the state variables are caused by changes in the perturbation.

$$X = [I_{L1} \ I_{L2} \ V_{C1} \ V_{C2}]^T \quad (9)$$

$$\dot{X} = Ax + Bu \quad (10)$$

Equations with small signal modeling that result are:

$$\dot{X} = [(A_1 - A_2)X + (B_1 - B_2)U]D \quad (11)$$

By calculating the values of matrixes,  $\mathbf{A}$ ,  $\mathbf{B}$  from Eq. (10) and Eq. (11), state space equations are as follows:

$$\begin{bmatrix} \dot{I}_{L1} \\ \dot{I}_{L2} \\ \dot{V}_{C1} \\ \dot{V}_{C2} \end{bmatrix}, A_1 = \begin{bmatrix} -R & 0 & D-1 & D \\ 0 & -R & D & D-1 \\ 1-D & -D & 0 & 0 \\ -D & 1-D & 0 & 0 \end{bmatrix} \begin{bmatrix} i_{L1} \\ i_{L2} \\ v_{C1} \\ v_{C2} \end{bmatrix} + \begin{bmatrix} 0 & 1/L \\ 0 & 0 \\ 0 & 0 \\ 0 & 0 \end{bmatrix} \begin{bmatrix} V_{C1} + V_{C2} - i_{out}R \\ V_{C1} + V_{C2} - i_{out}R \\ -I_{L1} - I_{L1} + i_{out} \\ -I_{L1} - I_{L2} + i_{out} \end{bmatrix} D \quad (12)$$

While operating the system, the parameters stated at the transfer function,  $I_{load}$ ,  $I_{L1}$ ,  $I_{L2}$ ,  $V_{C1}$ ,  $V_{C2}$  are accepted as stable parameters; however, qZSI depends on  $D$  as a factor to provide changes. Eq. (12) has been solved by implementing Laplace transform to determine current, voltages for inductor and capacitor respectively. The functions for capacitor voltage and inductor current can be solved as:

$$I_{L1}(s) - I_{L2}(s) = \frac{sC}{s^2 + RCs + 1} V_{in}(s) \quad (13)$$

$$V_{C1}(s) - V_{C2}(s) = \frac{1}{s^2 + RCs + 1} V_{in}(s) \quad (14)$$

According to Eq. (14), for the initial condition set out in Eq. (15), the characteristic equation of the qZSI related to  $V_{in}$  and total voltage of capacitors can be obtained as:

$$G_{V_{in}}^{V_{C1}+V_{C2}}(s) = \frac{(V_{C1} + V_{C2})(s)}{V_{in}(s)}; \\ D(s) = 0, i_{out}(s) = 0 \quad (15)$$

$$G_{V_{in}}^{V_{C1}+V_{C2}}(s) = \frac{1-2D}{LCs^2 + RCs + (1-2D)^2} \quad (16)$$

For DC-side modeling, the three-phase inverter bridge and external ac load are represented by a single switch and a current source connected in parallel [22]. The characteristic equation for the non-ideal q-ZSI is derived from small signal modeling as follows:

$$s^2 + \frac{R}{L}s + \frac{(1-2D)^2}{LC} = 0 \quad (17)$$

According to Eq. (10), the second order system equation is given as.

$$s^2 + 2\xi\omega_n s + \omega_n^2 = 0 \quad (18)$$

$\omega_n$  is calculated as.

$$\omega_n = 1 - D / \sqrt{LC} \quad (19)$$

And  $\xi$  is damping ratio and also calculated as:

$$\xi = \frac{R}{2(1-2D)} \sqrt{\frac{C}{L}} \quad (20)$$

From the expressions that are given above it clearly shows that the shoot through duty ratio, inductance and capacitance affects the system dynamic behavior.

## 3 CONTINUOUS TIME LEAST SQUARE ESTIMATION

It is impossible to determine the parameter estimation error since the parameters are unknown. Instead, the error between the actual signal and the reconstructed signal using estimated parameters is used [23]. After the nonlinear system was described as a polynomial equation, the model system parameters were calculated using the continuous time least squares technique. These polynomial equations are based on state-space analysis with small-signal modelling.

As the system has been accepted entirely, the system has run in continuous time, so parameter estimation has been carried out in continuous time, so  $\theta$  called estimated parameters, error of estimation is explained as at  $t$ ;

$$\varepsilon(t, \tau) = y(\tau) - \varphi(\tau)\theta(t) \quad (21)$$

The equation below seeks to reduce the error of estimation for the  $(t)$  vector and is a cost function that encompasses the optimization and linearization approach. Depending on the estimation error, if the error is the least, the system converges to the real system [22].

$$J(\theta(t), t) = e^{-\beta t} \cdot (\theta(t) - \theta_0)^T \cdot S_0 (\theta(t) - \theta_0) + + \int_0^t e^{-\beta(t-\tau)} \varepsilon^2(t, \tau) d\tau \quad (22)$$

where:

- $B$ , a constant coefficient that is greater than 0,
- $\theta_0$ , the initial parameter estimation vector, which is equal to 0,
- $S_0$  information matrix at the starting point expressed as  $\alpha I$ ,  $\alpha$  is near 0, and  $I$  is a unit matrix,
- $\theta(t)$  utilizing the cost function to estimate the error.

$$S(t) = e^{-\beta t} S_0 + \int_0^t e^{-\beta(t-\tau)} \varphi(\tau) \varphi(\tau)^T d\tau \quad (23)$$

is written as:

$$\theta(t) = S^{-1}(t) \left[ e^{-\beta t} S_0 \cdot \theta_0 + \int_0^t e^{-\beta(t-\tau)} \varphi(\tau) \varphi(\tau)^T d\tau \right] \quad (24)$$

where:

- $S(t)$  data matrix,
- $\theta(t)$ , vector of estimation parameter.

These two vectors identify the continuous time least square approach, and the information matrix is recursively arranged along with the parameters at  $t + h$ . In this scope, the parameter matrix is:

$$S(t+h) = e^{-\beta h} S(t) + \int_h^{t+h} e^{-\beta(t+h-\tau)} \varphi(\tau) \varphi(\tau)^T d\tau \quad (25)$$

$$\theta(t+h) = \theta(t) + S^{-1}(t+h) \int_t^{t+h} e^{-\beta(t+h-\tau)} \varphi(\tau) \varphi(\tau)^T \cdot \left[ y(\tau) - \varphi(\tau)^T \theta(t) d\tau \right] \quad (26)$$

where  $h$  is sampling range.

#### 4 CONTROL DESIGN OF QUASI Z SOURCE INVERTER

Several control techniques, such as nonlinear controllers and the traditional proportional-integral (PI) method, have been proposed for qZSI to attain fast dynamic response, good steady-state performance, and robustness against parameter variations [24]. As illustrated in Fig. 3, the control of the dc side and the ac side is examined individually. To operate the switches in the inverter section, the OR gate evaluates the signals produced by the dc-side control and the ac-side control for the dc-to-ac conversion together. By setting up the reference of total capacitor voltage to obtain expected outcomes, the overlap of  $D$  and  $M$  can be avoided. Total capacitor voltage  $V_{PN}$  is measured for dc-side control. The transfer function in Eq can be utilized to determine the

dynamics of  $V_{PN}$  produced by Eq. (16). By using small-signal modeling, the qZSI can be approximated linearly.

For linear approach, PI controller contributes the feedforward  $D$  with  $D_1$  which is applicable as the shoot-through compensator.  $D_0$  is satisfied depends on total voltage of capacitors  $V_{PN}$  and  $V_{in}$  in steady state.

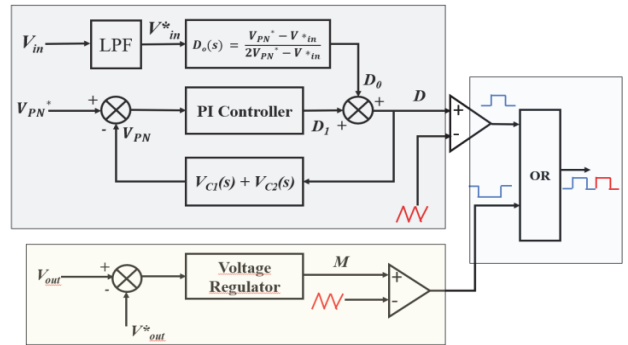


Figure 3 Controversial Feedforward PI Control Structure of qZSI

$$D_0(s) = \frac{V_{PN}^* - V_{in}^*}{2V_{PN}^* - V_{in}^*} \quad (27)$$

$V_{in}^*$  is the input voltage  $V_{in}$  after a low-pass filter. The whole capacitor voltage control loop's PI parameters can be determined via small-signal modelling. Traditional techniques are used to manage the voltage on the qZSI for the ac-side control. A simple PI compensator should be used to convert fundamental frequency from a three-phase system via  $d - q$  transformation method. This approach has been used in this paper.

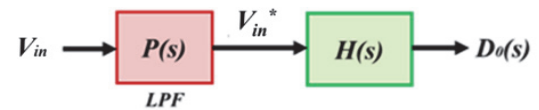


Figure 4 The diagram of generating  $d_0$  for qZSI

$$V_{in}^*(s) = V_{in} P(s) \quad (28)$$

The calculation of PI controller parameters could be difficult due to the values of capacitors and inductors. Instead of that, the characteristic in Eq. (16) is expressed as in Eq. (28) by approving a new parameter to characteristic equation. In order to optimize the parameters, CT-LSM is used and they are estimated. Subsequently, the PI controller parameters are easily calculated and implemented to proposed system.

$$G(s) = \frac{B_0}{A_0 s^2 + A_1 s + 1} \quad (29)$$

Based on estimated system parameters, within feedforward control, PI controller parameters have been satisfied by using Bode diagrams. Each estimated system parameter needs different PI control parameters to obtain ideal results.

The ideal  $V_{C1}$  and  $V_{C2}$  values are calculated using the input voltage over  $D$  obtained at the output under the dc side control. The system is controlled by comparing the sum of  $V_{C1}$  and  $V_{C2}$  with the assigned reference  $V_{PN}$ . The

control model of the ac side, the acquisition of the modulation signal is performed using conventional methods. The control design of the qZSI with the  $V_{PN}$  reference voltage block diagram is shown in Fig. 5.

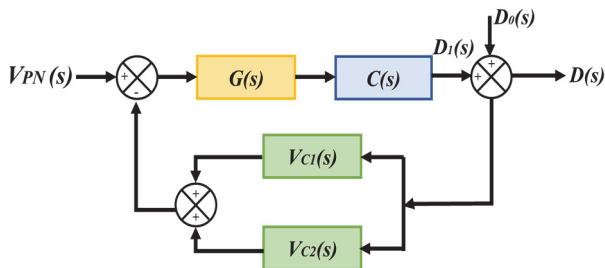


Figure 5 Control design of qZSI with  $V_{PN}$  reference voltage

Close loop transfer function according to Fig. 6 can be written as.

$$D_1(s) = G(s) \cdot C(s) \quad (30)$$

$$V_{C1}(s) = V_{in} \frac{1 - D(s)}{1 - 2D(s)} \quad (31)$$

$$V_{C2}(s) = V_{in} \frac{D(s)}{1 - 2D(s)} \quad (32)$$

$T(s)$  is written as using Eq. (30), Eq. (31) and Eq. (32) below:

$$T(s) = \frac{D_0(s) + D_1(s)}{1 + [D_0(s) + D_1(s)] \cdot [V_{C1}(s) + V_{C2}(s)]} \quad (33)$$

## 5 SIMULATION RESULTS

The values of the system parameters are listed in Tab. 1. According to the proposed control method, a system equation was suggested similar to Eq. (16).

Table 1 System design parameters

Design Parameters and Values	Values
QZS network (ideal conditions)	$L_1 = L_2 = L_3 = 500 \mu\text{H}$
	$C_1 = C_2 = 400 \mu\text{F}$
Output Filter	$L_f = 5 \text{ mH}$
	$C_f = 2.2 \mu\text{F}$
$R_{load}$	$10 \Omega$
Switching frequency ( $f_{sw}$ )	50 kHz
Reference frequency ( $f_r$ )	50 Hz
Input voltage ( $V_i$ )	220 Vrms

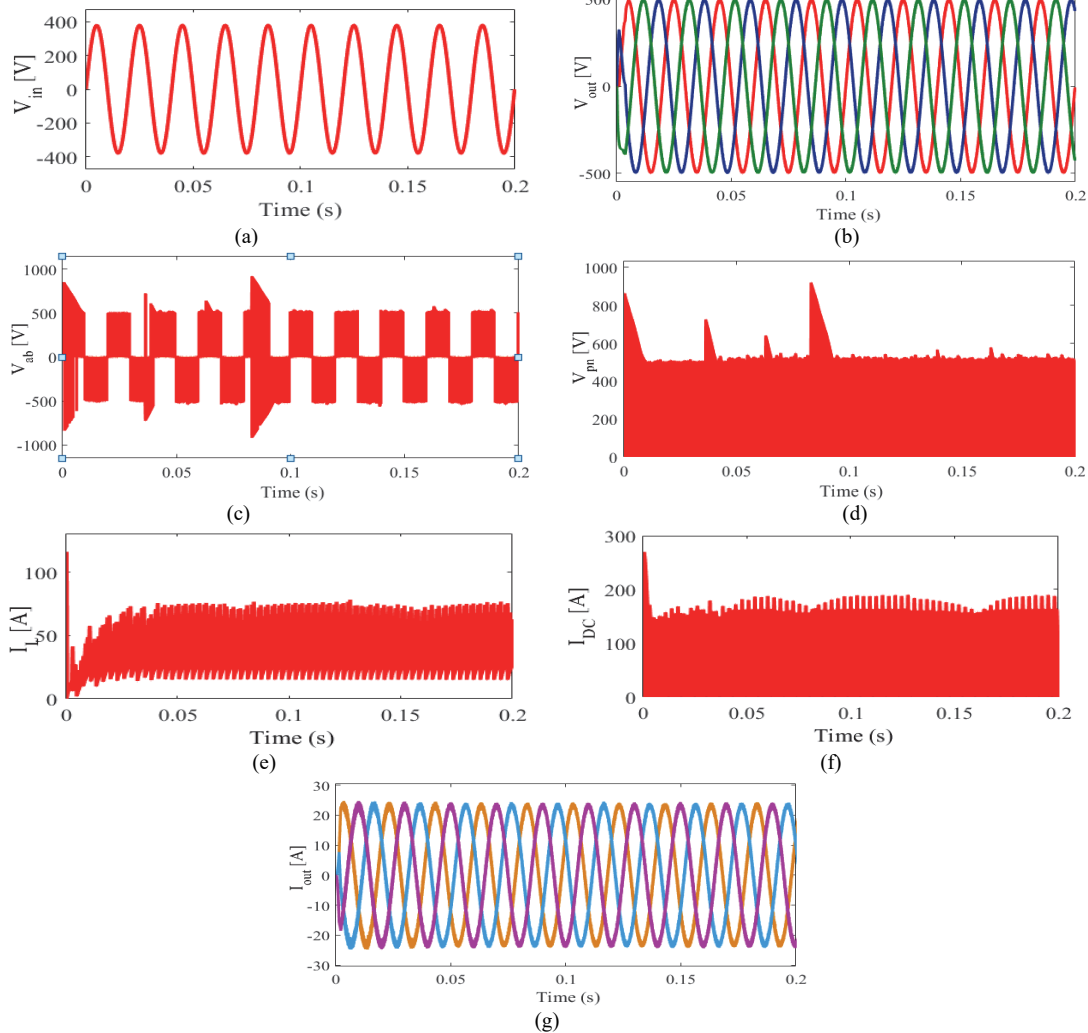


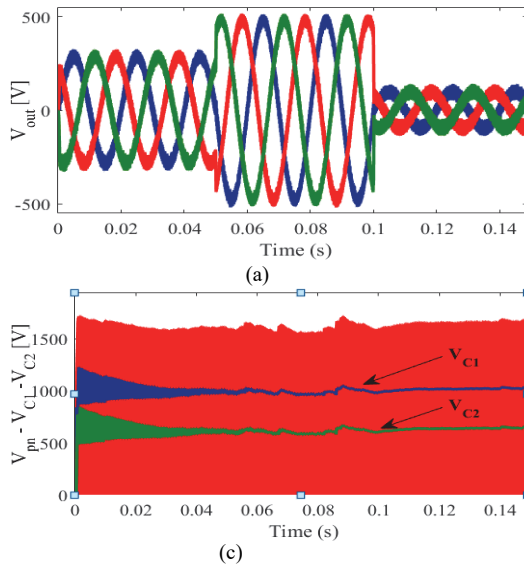
Figure 6 (a) System input voltage  $V_{in} = 220 \text{ V rms} \sim 380 \text{ V}$  (b) System output voltage (c) The voltage of switches for  $V_{ab}$  (d)  $V_{pn}$  voltage (e)  $I_L$  current on inductors. (f)  $I_{DC}$  DC-link current (g) Output current on load

Fig. 6 shows the steady-state responses of the dc and ac-side variables according to approved system equation. The results were obtained to load when  $V_{pn}$  and ac-side load voltage references were 500 V. The PI parameters on the dc side are calculated with a Bode diagram on Matlab. The PI parameters were calculated as  $K_p$ , 36 and  $K_I$ ,  $28 \times 10^{-4}$  for the dc side and  $K_p$ , 25 and  $K_I$ , 1 for the ac side. The responses are shown for  $10 \Omega$  in Fig. 6.  $V_{pn}$  was measured approximately 600 V, which implied that the boost factor ( $B$ ) and  $D$  values are approximately 1.80 and 0.22, respectively. Also, it was observed that the system output did not compensate for the phase shift that may occur in the output of the system.

The system parameters were estimated on Matlab based on parameter estimation algorithm by using Eq. (26). The equations of the estimated system equations at identified frequency ranges are listed in Tab. 2 and some samples are shown in Fig. 7.

**Table 2** Estimated system parameters

Approved System Equation	Sampling Range	Estimated System Equation
$\frac{1}{s^2 + 4s + 1}$	$h = 1$	$\frac{0.29}{0.88^2 + 1.62s + 1}$
	$h = 0.5$	$\frac{0.48}{1.44^2 + 2.28s + 1}$
	$h = 0.1$	$\frac{0.82}{2.48^2 + 3.43s + 1}$
	$h = 0.05$	$\frac{0.91}{2.72^2 + 3.68s + 1}$
	$h = 0.01$	$\frac{0.97}{2.92^2 + 3.91s + 1}$



**Figure 8** System Outputs for dynamic  $V_{ref}$  (a) Output load voltage (b) Output load current (c) Voltages in DC side (d) Currents in DC side

Fig. 8 shows the dynamic responses of the dc and ac variables for an abrupt change in the output reference voltage. The system was operated with new system equations, whose parameters were estimated with sampling range  $h = 0.01$ . The references for  $V_{pn}$ , PI control parameters, load, and  $V_{in}$  are given same as design criteria. The output reference voltage changes from 300 V<sub>AC</sub>, 500 V<sub>AC</sub> and 100 V<sub>AC</sub> respectively to observe buck-boost

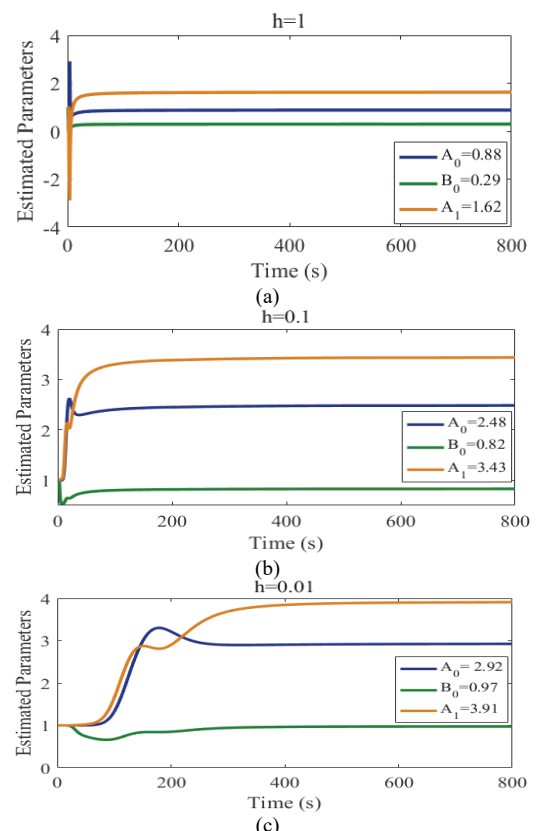
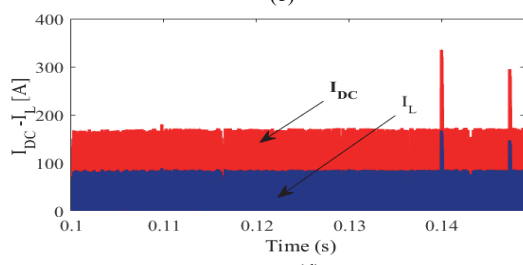
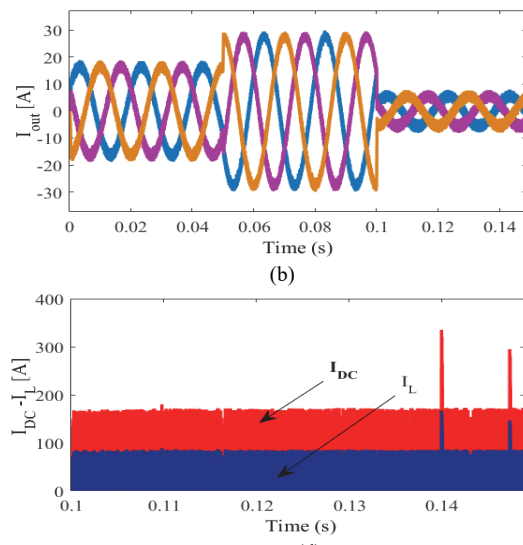


**Figure 7** Estimated Parameters a) for sampling range  $h = 1$  b) for sampling range  $h = 0.1$  c) for sampling range  $h = 0.01$



capabilities of the proposed system. The proposed system behaves successfully according to given output reference voltages in Fig. 8a.

The output current was changed from 10 A to 25 A, as shown in Fig. 8b. Both capacitor voltages on the dc side are maintained at a constant value, but the  $V_{pn}$  voltage has exceeded to its reference voltage and equals 1550 V in Fig. 8c. As a consequence of the output voltage change, the

inductor current and total current on the dc side increased, and spikes are observed in Fig. 8d. The calculated boost factor and  $D$  values were 2.27 and 0.372, respectively.

The behavior of the system estimated at a certain sampling interval with the proposed system is examined in Fig. 9. Here, it is seen that if the equation estimated for CT-LSM PI is applied at small sampling intervals, the total voltage explained as in related figure maximum value of  $V_{pn}$  to be transferred to the inverter part of the system increases and the boost factor increases accordingly. It has been observed that the proposed system is superior to PI control in terms of efficiency performance for qZSI.

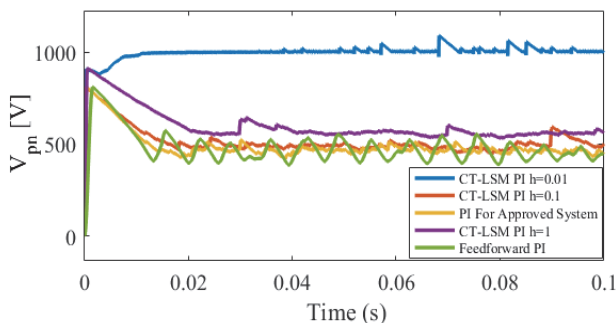


Figure 9 Comparison of stability and robustness for different systems

## 6 CONCLUSION

The CT-LSM PI control is designed and analyzed for the qZSI. This proposed control model provides enhanced boost for qZSI, higher voltage but increases capacitor voltage stress. That model also contributes to control such nonlinear systems without using real system parameters. In detail, the controller design and application of the proposed method are improved, including additional design stages required, if compared to the conventional PI methods, due to no need of estimation process for parameters in CT-LSM. Comparison results between PI control and CT-LSM PI control showed ideal steady-state behavior and high robustness of the qZSI using the proposed method. Some drawbacks are observed on dc side voltages, spikes in output currents when higher sampling ranges are used to estimate the system parameters. The potential of the proposed method is employed for industrial power applications for electrical motors and battery charging units connected to renewable energy resources such as solar systems. Future work will be conducted on eliminating the spikes and achieving wide input voltage intervals to develop efficiency for qZSI.

## 7 REFERENCES

- [1] Sehirli, E. & Cetinceviz, Y. (2022). Comparison of Average Current Controlled PFC SEPIC and CUK Converter Feeding Current Controlled SRM. *Tehnički Vjesnik*, 29(6), 1789-1795. <https://doi.org/10.17559/TV-20181108110207>
- [2] Zhao, J., Chen, D., & Jiang, J. J. (2021). A Novel Transformerless High Step-Up DC-DC Converter with Active Switched-Inductor and quasi-Z-Source Network. *WILEY IET Power Electronics*, 14(9), 1-14. <https://doi.org/10.1049/pel2.12128>
- [3] Pan, H. & Zhao, J. (2017). Quasi-Passivity-Based Adaptive Stabilization for Switched Nonlinearly Parameterized Systems. *WILEY International Journal Adaptive Control and Signal Processing*, 31(8), 1111–1125.
- [4] Bagheri, F., Komurcugil, H., Kukrer, O., Guler, N., & Bayhan, S. (2020). Multi-Input Multi-Output-Based Sliding-Mode Controller for Single-Phase Quasi-Z-Source Inverters. *IEEE Transactions on Industrial Electronics*, 67(8), 6439-6449. <https://doi.org/10.1109/TIE.2019.2938494>
- [5] Subhani, N., Kannan, R., Mahmud, A., & Blaabjerg, F. (2021). Z-source inverter topologies with switched Z-impedance networks: A review. *WILEY, IET Power Electronic*, 14(4), 727-750. <https://doi.org/10.1049/pel2.12064>
- [6] Sun, Q., Han, R., Zhang, H., Zhou, J., & Guerrero, J. M. (2015). A multiagent-based consensus algorithm for distributed coordinated control of distributed generators in the energy internet. *IEEE Transaction on Smart Grid*, 6(6), 3006-3019. <https://doi.org/10.1109/TSG.2015.2412779>
- [7] Dong, S., Zhang, Q., & Cheng, S. (2015). Analysis of critical inductance and capacitor voltage ripple for a bidirectional Z-source inverter. *IEEE Transaction on Power Electronics*, 30(7), 4009-4015. <https://doi.org/10.1109/TPEL.2014.2350991>
- [8] Priyadarshi, N., Padmanaban, S., Ionel, D., Mihet-Popa, L. & Azam, F. (2018). Hybrid PV-Wind, Micro-Grid Development Using Quasi-Z-Source Inverter Modeling and Control-Experimental Investigation. *Energies*, 11(9). <https://doi.org/10.3390/en11092277>
- [9] Zipeng, L., Sideng, H., Huan, Y., & Xiangning, H. (2018). Synthesis and Design of the AC Current Controller and Impedance Network for the Quasi-Z-Source Converter. *IEEE Transactions on Industrial Electronics*, 65(10), 8287-8296. <https://doi.org/10.1109/TIE.2018.2808928>
- [10] Ge, B., Liu, Y., Abu-Rub, H., Balog, R. S., Peng, F. Z., McConell, S., & Li, X. (2016). Current Ripple Damping Control to Minimize Impedance Network for Single-Phase Quasi-Z-Source Inverter System. *IEEE Transactions on Industrial Informatics*, 12(3), 1043-1054. <https://doi.org/10.1109/TII.2016.2544246>
- [11] Rehan, M. & Chughtai, A. H. (2020). Multicell Schemes for Active-Switched-Capacitor and Active-Switched-Capacitor/Switched Inductor Quasi-Z-Source Inverters. *IEEE Journal of Emerging and Selected Topics in Power Electronics*, 8(2), 1739-1754. <https://doi.org/10.1109/JESTPE.2019.2901689>
- [12] Zakipour, A., Kojori, S., & Tavakoli, B. (2017). Closed-loop control of the grid-connected Z-source inverter using hyperplane MIMO sliding mode. *IET Power Electronics*, 10(15), 2229-2241. <https://doi.org/10.1049/iet-pel.2017.0076>
- [13] Dong, K., Shi, T., Xiao, S., Li, X., & Xia, C. (2019). Finite set model predictive control method for quasi-Z source inverter-permanent magnet synchronous motor drive system. *IET Electric Power Applications*, 13(3), 302-309. <https://doi.org/10.1049/iet-epa.2018.5486>
- [14] Li, T. & Cheng, Q. (2019). Structure Analysis and Sliding Mode Control of New Dual quasi-Z-Source Inverter in Microgrid. *WILEY, International Transaction Electrical Energy Systems*, 29(1). <https://doi.org/10.1002/etep.2662>
- [15] Xiao, Z., Yuan, R., Chen, Y., Chen, Q., & Deng, X. (2014). Active power filter control strategy with novel dual-repetitive controller and neural network adaptive PI control. *Tehnički Vjesnik*, 21(3), 545-551.
- [16] Siwakoti, Y. P., Peng, F. Z., Blaabjerg, F., Loh, P. C., Town, G. E., & Yang, S. (2015). Impedance-source networks for electric power conversion part II: review of control and modulation techniques. *IEEE Transaction on Power Electronics*, 30(4), 1887-1906. <https://doi.org/10.1109/TPEL.2014.2329859>
- [17] Nguyen, M., Duong, T., Lim, Y. C., & Choi, J. H. (2019). High voltage gain quasi-switched boost inverters with low input current ripple. *IEEE Transaction on Industrial Electronics*, 15(9), 4857-4866. <https://doi.org/10.1109/TII.2018.2806933>

- [18] Ren, X. M., Rad, A. B., Chan, P. T., & Lo, W. L. (2005). Online identification of continuous-time systems with unknown time-delay. *IEEE Transaction Automatic Control*, 50(9), 1418-1422. <https://doi.org/10.1109/TAC.2005.854640>
- [19] Liu, C. Y., Loxton, R., & Teo, K. L. (2014). Optimal Parameter Selection for Nonlinear Multistage Systems with Time-Delays. *Computational Optimization and Applications*, 59, 285-306. <https://doi.org/10.1007/s10589-013-9632-x>.
- [20] Achlerkar, P. D. & Panigrahi, B. K. (2021). Recursive Least Squares-Based Adaptive Parameter Estimation Scheme for Signal Transformation and Grid Synchronization. *IEEE Journal of Emerging and Selected Topics in Power Electronics*, 9(2), 427-2439. <https://doi.org/10.1109/JESTPE.2020.2970445>
- [21] Liu, C., Han, M., Gong, Z., & Teo, K. L. (2021). Robust Parameter Estimation for Constrained Time-Delay Systems with Inexact Measurements. *Journal of Industrial and Management Optimization*, 17(1), 317-337. <https://doi.org/10.3934/jimo.2019113>
- [22] Shinde, U. K., Kadwane, S. G., Gawande, S. P., Reddy, M. J. B., & Mohanta, D. K. (2017). Sliding Mode Control of Single-Phase Grid-Connected Quasi-Z source Inverter. *IEEE Access*, 5, 10232–10240. <https://doi.org/10.1109/ACCESS.2017.2708720>
- [23] Chai, Q., Loxton, R., Teo, K. L., & Yang, C. H. (2013). A Unified Parameter Identification Method for Nonlinear Time-Delay Systems. *Journal of Industrial and Management Optimization*, 9(2), 471-486. <https://doi.org/10.3934/jimo.2013.9.471>
- [24] Zakiour, A., Kojori, S. S., & Bina, M. T. (2017). Closed-Loop Control of The Grid-Connected Z-Source Inverter Using Hyper-Plane MIMO Sliding Mode. *IET Power Electronics*, 10(15), 2229-2241. <https://doi.org/10.1049/iet-pel.2017.0076>

**Özkan ÖZKARA**, PhD Student

(Corresponding author)

Electrical and Electronics Engineering Department,  
Ankara Yıldırım Beyazıt University,  
Etilk/Keçören, Ankara, Turkiye  
E-mail: ozkan.ozkara@sanayi.gov.tr

**Ahmet KARAARSLAN**, PhD Lecturer

Electrical and Electronics Engineering Department,  
Ankara Yıldırım Beyazıt University,  
Etilk/Keçören, Ankara, Turkiye  
E-mail: akaraarslan@aybu.edu.tr